

Tensor meson photoproduction as a final state interaction effect

Łukasz Bibrzycki*

State School of Higher Education in Oświęcim, Kolbego 8, 32-600 Oświęcim, Poland

Robert Kamiński†

*Institute of Nuclear Physics, Polish Academy of Sciences,
Division of Theoretical Physics, 31-342 Kraków, Poland*

The model is presented to describe the $f_2(1270)$ meson photoproduction as a result of pion-pion interactions in the final state. Treating tensor mesons as objects dynamically created due to final state interactions is a convenient and straightforward way to employ data from $\pi\pi$ scattering like phase shifts and inelasticities for description of (photo)production reactions while retaining proper analytical structure of amplitudes, two particle unitarity and crossing symmetry. The model presented here can provide experimentally testable quantities like differential cross sections and $\pi\pi$ mass distributions as well as the strengths of partial waves corresponding to various $f_2(1270)$ helicities which are essential for partial wave analyses. It can also be used to compute moments of angular distribution and spin density matrix elements where partial wave interference effects are important.

PACS numbers: 13.60.Le, 13.75.-n, 13.60.-r, 14.40.-n

I. INTRODUCTION

Description of the spectrum of resonances observed in the $\pi\pi$ (and $K\bar{K}$) system and excited in photon nucleon collisions is one of the most challenging problems of hadron spectroscopy. In the diffractive region of high energies and low momentum transfers, this reaction is dominated by vector meson production generated by Pomeron exchange, and its theory is quite firm [1–3]. In the lower energies, the P -wave $\pi^+\pi^-$ photoproduction was described in terms of the t -channel exchange of Reggeons [4, 5]. Attempts have also been made to include the intermediate nucleon resonances through various s -channel and u -channel mechanisms [6–8]. For the photoproduction of the S -wave and D -wave resonances, the situation is not clear both experimentally and theoretically. Because of small photoproduction cross sections, they are very difficult to observe in mass distributions. So the method of choice is to analyze the interference patterns of the weak S - and D -wave amplitudes with dominant P -wave amplitude. The partial wave interference can be conveniently analyzed with moments of pion angular distribution or spin density matrix elements. Such an approach was employed in a recent analysis of the reaction $\gamma p \rightarrow \pi^+\pi^-p$ performed by the CLAS group at Jefferson Laboratory, where the first observation of $f_0(980)$ photoproduction was reported [9]. The same experiment saw the $f_2(1270)$ signal, which previously was also observed by Hermes experiment at Deutsches Elektronen-Synchrotron using similar methods [10]. The apparent sensitivity of moments analysis in the search for a sig-

nal of rare resonances has a reverse, however, namely, that it requires proper accounting for all relevant production mechanisms. Nevertheless this method has been successfully employed to extract the $f_0(980)$ and $a_0(980)$ from the photoproduced $K\bar{K}$ spectrum [11] and $f_0(980)$ from the $\pi^+\pi^-$ spectrum [12]. The amplitude of $f_2(1270)$ photoproduction is the necessary ingredient in order to properly describe the partial wave interference pattern for $\pi\pi$ effective masses above 1 GeV.

Previously, the electromagnetic processes involving tensor mesons were described in terms of the combined tensor meson dominance and vector meson dominance models [5, 13, 14], Regge inspired exchange models [15, 16], or effective field theories [17, 18]. None of these approaches can, however, be treated as properly tested in tensor meson photoproduction on a nucleon. Production of $f_2(1270)$ has been extensively analyzed in other reactions like $\gamma\gamma \rightarrow \pi^+\pi^-$ and $\gamma\gamma \rightarrow \pi^0\pi^0$ [19, 20]. The authors of these studies found that this resonance is dominantly produced in quark-antiquark channel and that pion-pion final state interactions are negligible. We note, however, that qualitative characteristics of the $\gamma\gamma \rightarrow \pi\pi$ reaction are quite different from those of $\gamma p \rightarrow \pi^+\pi^-p$ photoproduction. For example, the $f_0(980)$ signal which is relatively small yet clear in $\gamma\gamma \rightarrow \pi\pi$ reaction analyzed by Belle [21] is completely absent in $\pi^+\pi^-$ mass distribution of $\gamma p \rightarrow \pi^+\pi^-p$ reaction measured by CLAS, even though the data errors and mass resolution of 10 MeV are in principle sufficient to observe it (see eg. Fig. 4 of [9]). It was only due to $f_0(980)$ interference with the dominant P -wave that the $f_0(980)$ has been observed. On the other hand, in the $\pi^+\pi^-$ and $\pi^0\pi^0$ mass distributions measured by Belle Collaboration [21], the $f_2(1270)$ signal hugely outnumbers the $f_0(980)$ one. This is in contrast with the mass distributions of the S - and D -waves measured by CLAS and integrated in the neighborhood of the $f_0(980)$ and $f_2(1270)$ resonances for the $\gamma p \rightarrow \pi^+\pi^-p$ re-

* Corresponding author.
lukasz.bibrzycki@ifj.edu.pl

† Corresponding author.
robert.kaminski@ifj.edu.pl

action. In this measurement, the $f_0(980)$ cross section is smaller than the $f_2(1270)$ one only by a factor of about 4 (see figs. 22 and 24 of [9]). We also stress that our approach does not contradict the $q\bar{q}$ nature of the $f_2(1270)$ resonance. This is because the $\pi\pi$ amplitudes which we use as the input were derived in the model independent way. Moreover, our assumptions concerning the meson exchanges included in Born amplitudes can be directly checked by comparison of model predictions with precision data on partial wave interference in the $\pi\pi$ effective mass range corresponding to the $f_2(1270)$ resonance.

In what follows, we will refer to $\pi^+\pi^-$ photoproduction as description of D -wave data from CLAS is our main objective. One has to mention, however, that the formalism we present is *mutatis mutandis* applicable to $\pi^0\pi^0$ photoproduction.

II. MODEL FOR THE $\pi^+\pi^-$ PHOTOPRODUCTION

A. Born amplitudes

In our approach the tensor meson photoproduction is treated as a two-stage phenomenon. First, a pair of pions is photoproduced. According to Regge phenomenology, this process at high energies should be dominated by t -channel ρ and ω exchanges. Then pions undergo the final state interactions which may result in the resonance creation. This two-stage process is schematically drawn in Fig.1. The principal merit of the model we propose is that it preserves important features of the $\pi\pi$ scattering amplitudes described in Sec. IIB like two-particle unitarity, proper analytical structure, and crossing symmetry and embeds them seamlessly in the framework of the photoproduction amplitude. We follow the general

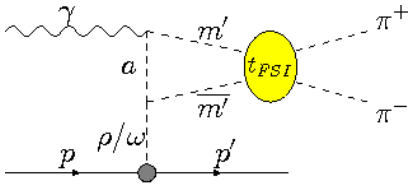


FIG. 1. The diagram of two pion photoproduction with final state interactions where a denotes π , ρ or ω .

formalism of Refs. [22, 23] but specialize the results to the case of two pions photoproduced in the D -wave (for completeness we will recall some important formulas of these references). The amplitude of the final state interactions is described in [24, 25]. In principle, our approach does not engage any new parameters, as coupling constants and form factor range parameters are common for all partial waves and the same as in [22]. The vector meson to nucleon couplings are taken from Bonn model [26] and so is the monopole form factor used in VNN

vertex. In practice, however, the cross sections computed with these parameters substantially overestimate the experimentally measured data. So we leave ourselves with the freedom to use the overall rescaling factor to adjust the cross section predicted by the model to experimental data. Thus, we treat the relative strengths of partial waves corresponding to different angular momentum projections as the principal model prediction. These depend mainly on the meson exchanges taken into account in the model. We believe that any possible variations of couplings will not change the picture presented here substantially. Predictions for partial wave amplitude strengths (and phases) are important components for analysis of moments of $\pi^+\pi^-$ angular distribution. This analysis will be discussed in the paper to follow [27] with application of amplitudes discussed here. Our calculations are performed in the helicity system which is the center of the mass system of the two photoproduced pions. In this system the z -axis is directed opposite to final proton momentum \mathbf{p}' , the y -axis is perpendicular to the production plane, and the x -axis vector is defined as $\hat{x} = \hat{y} \times \hat{z}$. We describe the initial state $\pi\pi$ photoproduction in terms of Born amplitudes derived from the phenomenological Lagrangian:

$$\mathcal{L} = \mathcal{L}_{\pi\pi\gamma} + \mathcal{L}_{\rho\pi\gamma} + \mathcal{L}_{\omega\pi\gamma} + \mathcal{L}_{\rho\pi\pi\gamma} + \mathcal{L}_{\rho\pi\pi} + \mathcal{L}_{\rho\pi\omega} + \mathcal{L}_{\omega NN} + \mathcal{L}_{\rho NN}, \quad (1)$$

where individual terms of Eq.(1) are defined in [22]. The diagram representation of amplitudes obtained from this Lagrangian is shown in Fig.2 and they have a general form of

$$V_{m\bar{m}} = \sum_{r=I,II} \bar{u}(p', s') J_{r, m\bar{m}} \cdot \varepsilon(q, \lambda_\gamma) u(p, s), \quad (2)$$

where $J_{r, m\bar{m}}$ is the hadronic current, $u(p, s)$ and $\bar{u}(p', s')$ - wave functions of the initial and final proton, respectively, and ε the polarization vector of the incident photon which reads

$$\varepsilon(q, \lambda_\gamma) = (0, \varepsilon^{\lambda_\gamma}), \quad (3)$$

where

$$\varepsilon^{\lambda_\gamma} = -\frac{\lambda_\gamma}{\sqrt{2}} (\cos \theta_q, i\lambda_\gamma, \sin \theta_q) \quad (4)$$

and λ_γ is photon helicity. The photon polarization vector is transverse to photon momentum:

$$\mathbf{q} = |\mathbf{q}|(-\sin \theta_q, 0, \cos \theta_q), \quad (5)$$

and

$$\cos \theta_q = \frac{E^2 - E'^2 - |\mathbf{q}|^2}{2|\mathbf{q}||\mathbf{p}'|}. \quad (6)$$

The energies E and E' of the initial and final proton respectively, as well as photon energy $|\mathbf{q}|$ can be expressed in terms of Lorentz invariant quantities:

$$E = \frac{s - m^2 + t}{2M_{\pi\pi}}, \quad E' = \frac{s - m^2 - M_{\pi\pi}^2}{2M_{\pi\pi}}, \quad (7)$$

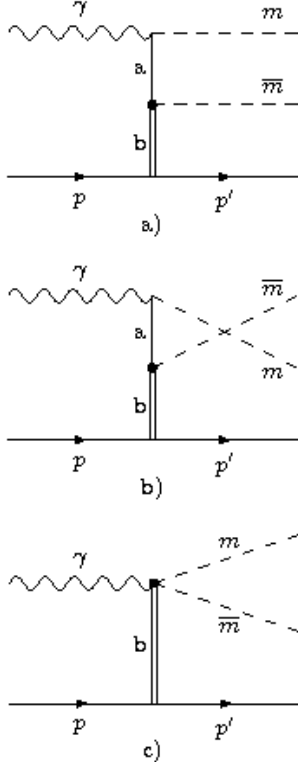


FIG. 2. The structure of diagrams corresponding to Born photoproduction amplitudes

$$|q| = \frac{M_{\pi\pi}}{2} - \frac{t}{2M_{\pi\pi}}, \quad (8)$$

where s is the γp energy squared, t is the square of the 4-momentum transfer from initial photon to the photo-produced $\pi\pi$ system, m is the proton mass and $M_{\pi\pi}$ is the effective mass of two pions.

In Eq.(2) $r = I$ corresponds to the sum over diagrams where $a = \pi$ in Fig.2 (including the contact diagram) and $r = II$ corresponds to the sum of diagrams with $a = \rho$ or ω . The summary of these diagrams is shown in Table I. The amplitude defined in Eq.(2) is then D -wave

$m\bar{m}$	$r=I$	$r=II$
$\pi^+\pi^-$	$(a, b) = (\pi^\pm, \rho^0)$	$(a, b) = (\rho^\pm, \omega)$
$\pi^0\pi^0$		$(\rho^0, \omega), (\omega, \rho^0)$

TABLE I. Summary of meson exchanges in Born amplitudes.

projected using the formula:

$$V_{m\bar{m}}^{2M} = \frac{1}{\sqrt{4\pi}} \int d\Omega Y_M^{2*}(\Omega) V_{m\bar{m}}. \quad (9)$$

In our frame of reference, the momenta of photoproduced pions can be expressed in terms of the solid angle Ω , i.e., $\mathbf{k}_1 = -\mathbf{k}_2 = |k|\hat{\kappa}(\Omega)$. $\mathbf{k}_1(\mathbf{k}_2)$ is the positive (negative) pion momentum and $\hat{\kappa} = (\sin\theta \cos\varphi, \sin\theta \sin\varphi, \cos\theta)$. In

what follows we will write just k instead of $|k|$ for brevity. The general form of the current used in Eq.(2) is

$$J_{r,m\bar{m}}^\mu = (\alpha_{r,m\bar{m}} g^{\mu\nu} + k_1^\mu \beta_{1r,m\bar{m}}^\nu + k_2^\mu \beta_{2r,m\bar{m}}^\nu) \times \{d_{r,m\bar{m}} \gamma_\nu + e_{r,m\bar{m}}(p + p')_\nu\} \quad (10)$$

where functions $\alpha_{r,m\bar{m}}$, $\beta_{1r,m\bar{m}}$, $\beta_{2r,m\bar{m}}$, $d_{r,m\bar{m}}$ and $e_{r,m\bar{m}}$ are defined in [22]. It is interesting to note that terms of Eq.(10) contained in curly braces do not depend on pion momenta, and thus they can be factorized out of the partial wave expansion. Physically, it means that in this model the D -wave angular momentum projections M are uncorrelated with nucleon spin projections. Finally, after all pion momentum independent terms are factorized out of Eq.(9) we arrive at the D -wave projected tensor defined as

$$P_{r,m\bar{m}}^{2M,\mu\nu} = \frac{1}{\sqrt{4\pi}} \int d\Omega Y_M^{2*}(\Omega) (\alpha_{r,m\bar{m}} g^{\mu\nu} + k_1^\mu \beta_{1r,m\bar{m}}^\nu + k_2^\mu \beta_{2r,m\bar{m}}^\nu). \quad (11)$$

Because of the photon polarization vector definition [Eq.(3)], the only matrix elements of the tensor $P_{r,m\bar{m}}^{2M}$ which enter the amplitude are $P_{r,m\bar{m}}^{2M,i0}$ and $P_{r,m\bar{m}}^{2M,ij}$, where $i, j = x, y, z$. We stress that the form of the tensor $P_{r,m\bar{m}}^{2M}$ is general and it can be used to construct other amplitudes to describe transition of two vector particles into two pseudoscalar ones, e.g. $\gamma\gamma^* \rightarrow m\bar{m}$, where $m\bar{m}$ can be $\pi\pi$, $K\bar{K}$, $\pi\eta$. Therefore the full expressions for individual matrix elements of the tensor $P_{r,m\bar{m}}^{2M}$ for $r = I$ and $r = II$ are given in the Appendix.

B. Final state scattering amplitudes

The $\pi\pi$ final state scattering amplitudes $t_\ell^I(s_{\pi\pi}) = t_2^0(s_{\pi\pi})$ and $t_2^2(s_{\pi\pi})$ for the D wave with isospin 0 and 2 respectively, have been described using parameterization constructed and used in the recent dispersive data analysis [24]. Their advantage over other parameterizations is unitarity, analyticity and model independent formalism. The D -wave amplitudes have been fitted to experimental data up to 1.42 GeV and indirectly to a system of dispersion relations below 1.1 GeV. Two of these relations were the Roy like ones, i.e., relations with imposed crossing symmetry condition. One of them, presented and called for short GKPY in [24], has been derived with one subtraction and proved to be very demanding which allowed for very precise determination of directly fitted amplitudes (S and P) and, indirectly, other ones (D , F and G). The general form of dispersion relations with one subtraction for the D -wave amplitudes reads:

$$\text{Re } t_2^I(s_{\pi\pi}) = d_2^I(s_{\pi\pi}) + \sum_{I'=0}^2 \sum_{\ell'=0}^3 \int_{4m_\pi^2}^{s'_{\pi\pi;max}} ds'_{\pi\pi} K_{2\ell'}^{II'}(s_{\pi\pi}, s'_{\pi\pi}) \text{Im } t_{\ell'}^{I'}(s'_{\pi\pi}) \quad (12)$$

where $I = 0, 2$, $s_{\pi\pi} = M_{\pi\pi}^2$, $s'_{\pi\pi;max} = 1.42 \text{ GeV}^2$, and the factors $K_{2\ell'}^{II'}(s_{\pi\pi}, s'_{\pi\pi})$ are kernels derived with an imposed crossing symmetry condition. Terms $d_2^I(s_{\pi\pi})$ comprise contributions from all partial waves above $s'_{\pi\pi} = s'_{\pi\pi;max}$ where the input amplitudes are described by using the Regge formalism. Below $s'_{\pi\pi} = s'_{\pi\pi;max}$, all partial wave amplitudes $t_{\ell'}^{I'}(s'_{\pi\pi})$ are parameterized by using simple polynomials for phase shifts $\delta(s'_{\pi\pi})$ and inelasticities $\eta(s'_{\pi\pi})$ which guarantees their unitarity; see [24] for details. These amplitudes can be expressed by experimental $\delta_{\ell'}^{I'}(s_{\pi\pi})$ and $\eta_{\ell'}^{I'}(s_{\pi\pi})$:

$$t_{\ell'}^{I'}(s'_{\pi\pi}) = \frac{s'_{\pi\pi}(\eta_{\ell'}^{I'}(s_{\pi\pi})e^{i\delta_{\ell'}^{I'}(s_{\pi\pi})} - 1)}{2i\sqrt{s'_{\pi\pi} - 4m_\pi^2}}. \quad (13)$$

For the isoscalar D wave, these are of course dominated by the $f_2(1270)$ resonance.

As has been presented in [25], although the D -wave amplitudes were not fitted directly to the GKPY dispersion relations, they very well fulfill crossing symmetry condition below about 0.8 GeV and quite well above this

energy.

Another argument in favor of our choice of parameterization was that (see [24, 25]), although all amplitudes (S - G partial waves) have been fitted separately to their "own" data, they all had to be related with each other in very wide energy range via simultaneous fit to the S and P waves. These mutual relations are due to theoretical crossing symmetry condition imposed on the amplitudes in the Roy and GKPY equations. It guarantees mutual consistency of all partial wave amplitudes and allows to believe that isoscalar D wave amplitude will not need any sizable further modifications in future.

C. Complete photoproduction amplitudes

The complete (i.e. including the final state interactions) amplitude of the D -wave $\pi^+\pi^-$ photoproduction contains the information on energy and momentum transfer dependence of $\pi\pi$ photoproduction as well as the pion momentum (or effective mass) dependence of the $\pi\pi$ scattering amplitude with proper analytical structure encoded. It reads

$$\begin{aligned} \langle \lambda' M | A_{\pi^+\pi^-} | \lambda_\gamma \lambda \rangle &= \langle \lambda' M | \hat{V}_{\pi^+\pi^-} | \lambda_\gamma \lambda \rangle \\ &+ 4\pi \sum_{m'\bar{m}'} \int_0^\infty \frac{k'^2 dk'}{(2\pi)^3} F(k, k') \langle \pi^+\pi^- | \hat{t}_{FSI} | m'\bar{m}' \rangle G_{m'\bar{m}'}(M'_{\pi\pi}) \langle \lambda' M | \hat{V}_{m'\bar{m}'} | \lambda_\gamma \lambda \rangle \end{aligned} \quad (14)$$

where \hat{V} is the Born amplitude of the $\pi^+\pi^-$ or $\pi^0\pi^0$ photoproduction, \hat{t}_{FSI} is the $\pi\pi$ scattering amplitude, $\lambda, \lambda', \lambda_\gamma$ and M are, respectively, the helicities of the initial and final proton, photon helicity, and projection of the $\pi\pi$ system angular momentum on the spin quantization axis z [which can be identified with the $f_2(1270)$ helicity]. \hat{G} is the propagator of the intermediate pion pair and reads

$$G_{m'\bar{m}'}(M'_{\pi\pi}) = \frac{1}{M_{\pi\pi} - M'_{\pi\pi}(k') + i\varepsilon}. \quad (15)$$

$F(k, k')$ is the form-factor needed to regularize divergent mesonic loop of diagram shown in Fig.1. Results obtained in the S -wave calculations [22] suggest that the particular value of this form-factor cut-off parameter may strongly affect calculated cross sections, and thus it should be carefully fitted to the data. In this explanatory study we limit ourselves to the on-shell part of the amplitude and leave the problem of fitting the form-factor parameter for further investigation. After integration and rewriting the $\pi\pi$ amplitude in terms of isospin

amplitudes, we arrive at the following expression:

$$\begin{aligned} \langle \lambda' M | \hat{A}_{\pi^+\pi^-} | \lambda_\gamma \lambda \rangle &= \\ [1 + ir_\pi \left(\frac{2}{3} t_{\pi\pi}^{I=0} + \frac{1}{3} t_{\pi\pi}^{I=2} \right)] \langle \lambda' M | \hat{V}_{\pi^+\pi^-} | \lambda_\gamma \lambda \rangle &+ \\ + \frac{1}{3} [ir_\pi (-t_{\pi\pi}^{I=0} + t_{\pi\pi}^{I=2})] \langle \lambda' M | \hat{V}_{\pi^0\pi^0} | \lambda_\gamma \lambda \rangle, \end{aligned} \quad (16)$$

where $r_\pi = -kM_{\pi\pi}/8\pi$. First term in Eq.(16) describes fully elastic scattering, while the second term is the recharging term with a pair of neutral pions in the intermediate state converted to $\pi^+\pi^-$ in the final state.

III. RESULTS

We have calculated the double differential cross section using the same formula as in [22]. Out of 40 spin amplitudes describing the D -wave $\pi\pi$ photoproduction only 20 are independent due to amplitude invariance under parity transformation. So we choose the photon helicity $\lambda_\gamma = +1$ as a reference helicity and refer to amplitudes corresponding to various M as no flip, single flip (either up or down), double flip amplitudes and so forth. From Eq.(14) we see that strengths of the photoproduction amplitudes with different M *entirely* depend on the

Born amplitudes and that final state interactions modulate these amplitudes uniformly. Moreover, the full photoproduction amplitude consists of the part proportional to $V_{\pi^+\pi^-}$ and $V_{\pi^0\pi^0}$. So it is interesting to know the Born cross sections of individual partial waves for both charged and neutral pion pairs. We show these cross sections in Figs. 3 and 4. It is worth mentioning that,

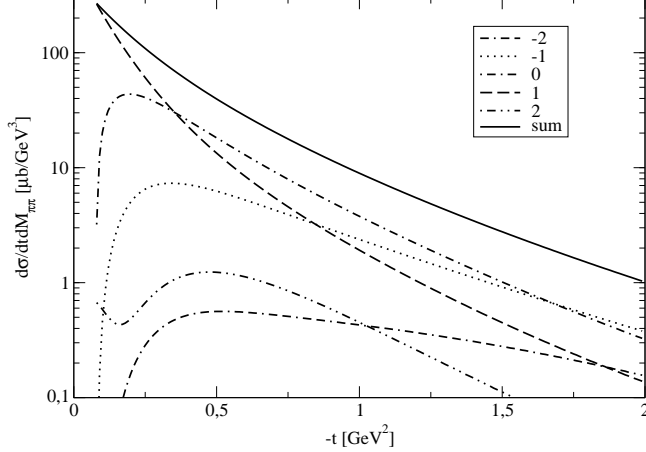


FIG. 3. Born cross sections for $\pi^+\pi^-$ photoproduction at $E_\gamma=3.5$ GeV and $M_{\pi\pi}=1.27$ GeV for different angular momentum projections (see legend).

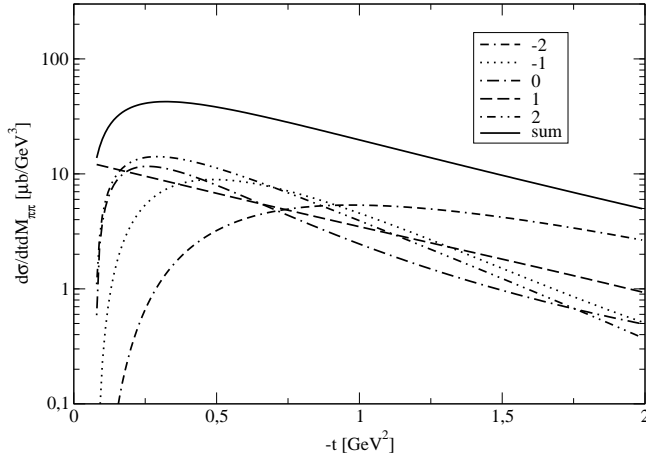


FIG. 4. Born cross sections for $\pi^0\pi^0$ photoproduction at $E_\gamma=3.5$ GeV and $M_{\pi\pi}=1.27$ GeV for different angular momentum projections (see legend).

while $\pi^+\pi^-$ photoproduction is dominated by contributions of $M = +1, 0$ and -1 (dashed, dot-dashed and dotted curves in Fig.3), $\pi^0\pi^0$ photoproduction has strong contributions of partial waves corresponding to $M = \pm 2$ (dot-dot-dashed and dash-dash-dotted curves, respectively, in Fig.4). It can be understood as a consequence of double vector meson exchange, as the Born amplitudes for $\pi^0\pi^0$ photoproduction are only type II amplitudes. On the other hand, the Born amplitudes for $\pi^+\pi^-$ photoproduction have both type I and type II contributions with

dominating type I contribution.

In Figs. 5 and 6, we show the D -wave mass distribution as well as mass distributions for $M=-1, 0, +1$ compared with the corresponding data from CLAS. The model

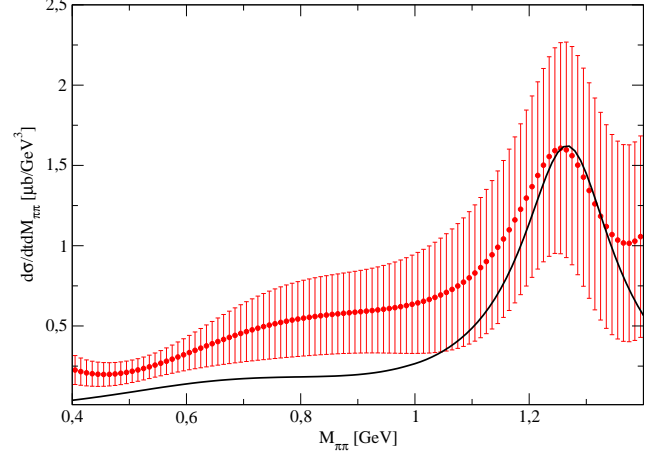


FIG. 5. Model prediction for D -wave $\pi^+\pi^-$ mass distribution at $E_\gamma = 3.3$ GeV and $-t=0.55$ GeV² compared to CLAS data (color online).

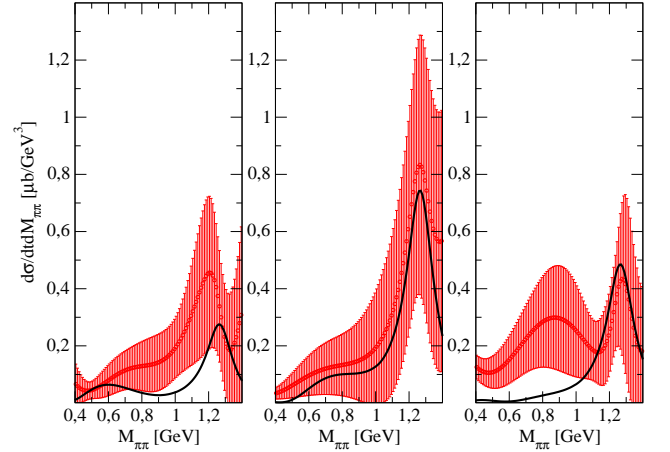


FIG. 6. Model prediction for $\pi^+\pi^-$ mass distribution for $M=-1$ (left panel), $M=0$ (middle panel) and $M=+1$ (right panel) at $E_\gamma = 3.3$ GeV and $-t=0.55$ GeV² compared to CLAS data (color online).

quite well reproduces the shape of the resonance. The slight asymmetry of the resonance and shift of its maximum towards lower masses observed in the experiment may be attributed to the interference of the resonant D -wave amplitude with flat contribution of other mechanisms involving pion-nucleon rescattering (Drell mechanism). This feature will be accounted for in further studies [27]. Another striking feature of mass distributions corresponding to different values of angular momentum projection is that, contrary to vector meson photoproduction where the dominating M coincided with the helicity of incident photon ($+1$ in our convention) in wide

range of momentum transfers, D -wave photoproduction is dominated by $M = 0$ amplitude. Our model very well reproduces this feature. Moreover, for $\pi^+\pi^-$ photoproduction it predicts small strengths of the partial waves corresponding to $M = \pm 2$ (they amount to 3.3% and 1.6% of the total D -wave intensity, respectively). This is in agreement with common practice in experimental analyses, where amplitudes with $|M| > 1$ are neglected [9, 28, 29]. We stress, however, that this assumption is not true for $\pi^0\pi^0$ where contributions of partial waves with $M=2$ are significant.

In actual calculations, we have adopted the definition of [30] and added the factor i to numerator of the propagator (Eq.(15)) used in the isoscalar part of the amplitude. This reflects the fact that the isoscalar amplitude describes the correlated (resonating) pion pair of spin 2. On the other hand, the isotensor amplitude describes two uncorrelated pions which essentially propagate independently, thus giving the overall factor of -1. This heuristic argument can be substituted in phenomenological applications by introducing an additional correction phase between $I=0$ and $I=2$ amplitudes and treating it as a model parameter.

IV. DISCUSSION AND OUTLOOK

We have presented the theoretical description of the $\pi^+\pi^-$ photoproduction in D -wave, treating the resonant behavior of the amplitude as due to pion-pion final state interactions. In this explanatory study we limited ourselves to the on-shell part of the amplitude, leaving the analysis of the off-shell effects for further study. S -wave analyses suggest that off-shell effects can be strong in

fact, but proper fixing of the cut-off parameter requires careful fitting to the data and thus accounting for other mechanisms contributing to the D -wave amplitude (like Drell mechanism). This will be the subject of our further study. The model properly reproduces relative strengths of different partial waves and, in particular, the fact that the mass distribution in resonance region is dominated by the $M=0$ partial wave. Additional check of the model predictions will be the calculation of moments of pion angular distribution and comparison with moments measured by CLAS experiment.

ACKNOWLEDGMENTS

This work has been supported by the Polish Ministry of Science and Higher Education (grant No N N202 236940).

Appendix: Matrix elements of the tensor $P_{r,m\bar{m}}^{2M}$

In this Appendix, we present the detailed form of the D -wave projected elements of the $P_{r,m\bar{m}}^{2M}$ tensor for both type I and type II amplitudes. The spherical harmonics $Y_m^{l*}(\hat{q})$ used below are understood as $Y_m^{l*}(\hat{q}) = Y_m^l(\cos\theta_q, \varphi_q = \pi)$. This results from the definition of the photon vector by Eq.(5). In formulas below the off-diagonal, spacial (ie. $i \neq 0$ and $j \neq 0$) tensor elements are split into nonsymmetric and symmetric parts $P_r^{2M,ij} = N_r^{2M,ij} + S_r^{2M,ij}$ for both type I and II amplitudes. For type I amplitudes the tensor components read (we omit the $m\bar{m}$ subscript for brevity):

$$P_I^{2M,x0} = -\sqrt{2}\sqrt{\frac{4\pi}{3}} \sum_{l=0}^3 \sum_{m=-l}^l \sqrt{3 \cdot (2l+1) \cdot 5} \begin{pmatrix} 1 & l & 2 \\ 0 & 0 & 0 \end{pmatrix} \left[\begin{pmatrix} 1 & l & 2 \\ -1 & m & M \end{pmatrix} - \begin{pmatrix} 1 & l & 2 \\ +1 & m & M \end{pmatrix} \right] Y_m^{l*}(\hat{q}) Q_l(x), \quad (\text{A.1})$$

$$P_I^{2M,y0} = -\sqrt{2}i\sqrt{\frac{4\pi}{3}} \sum_{l=0}^3 \sum_{m=-l}^l \sqrt{3 \cdot (2l+1) \cdot 5} \begin{pmatrix} 1 & l & 2 \\ 0 & 0 & 0 \end{pmatrix} \left[\begin{pmatrix} 1 & l & 2 \\ +1 & m & M \end{pmatrix} + \begin{pmatrix} 1 & l & 2 \\ -1 & m & M \end{pmatrix} \right] Y_m^{l*}(\hat{q}) Q_l(x), \quad (\text{A.2})$$

$$P_I^{2M,z0} = -2\sqrt{\frac{4\pi}{3}} \sum_{l=0}^3 \sum_{m=-l}^l \sqrt{3 \cdot (2l+1) \cdot 5} \begin{pmatrix} 1 & l & 2 \\ 0 & 0 & 0 \end{pmatrix} \begin{pmatrix} 1 & l & 2 \\ 0 & m & M \end{pmatrix} Y_m^{l*}(\hat{q}) Q_l(x), \quad (\text{A.3})$$

$$P_I^{2M,xx} = P_{I;1}^{2M,xx} + P_{I;2}^{2M,xx}, \quad (\text{A.4})$$

where

$$P_{I;1}^{2M,xx} = -\sqrt{2}\sqrt{\frac{4\pi}{3}} \sum_{l=0}^3 \sum_{m=-l}^l \sqrt{3 \cdot (2l+1) \cdot 5} \begin{pmatrix} 1 & l & 2 \\ 0 & 0 & 0 \end{pmatrix} \left[\begin{pmatrix} 1 & l & 2 \\ -1 & m & M \end{pmatrix} - \begin{pmatrix} 1 & l & 2 \\ +1 & m & M \end{pmatrix} \right] Y_m^{l*}(\hat{q}) Q_l(x) \hat{q}^x,$$

$$P_{I;2}^{2M,xx} = 4\sqrt{\frac{4\pi}{6}} \frac{k}{|q|} \sum_{l=0}^4 \sum_{m=-l}^l \left\{ \sqrt{\frac{2}{3}} \sqrt{1 \cdot (2l+1) \cdot 5} \begin{pmatrix} 0 & l & 2 \\ 0 & 0 & 0 \end{pmatrix} \begin{pmatrix} 0 & l & 2 \\ 0 & m & M \end{pmatrix} + \frac{1}{\sqrt{5}} \sqrt{5 \cdot (2l+1) \cdot 5} \begin{pmatrix} 2 & l & 2 \\ 0 & 0 & 0 \end{pmatrix} \right. \\ \left. \left[\begin{pmatrix} 2 & l & 2 \\ -2 & m & M \end{pmatrix} + \begin{pmatrix} 2 & l & 2 \\ +2 & m & M \end{pmatrix} - \sqrt{\frac{2}{3}} \begin{pmatrix} 2 & l & 2 \\ 0 & m & M \end{pmatrix} \right] \right\} Y_m^{l*}(\hat{q}) Q_l(x),$$

$$N_I^{2M,xy} = 0, \quad (\text{A.5})$$

$$S_I^{2M,xy} = 4i\sqrt{\frac{4\pi}{30}} \frac{k}{|q|} \sum_{l=0}^4 \sum_{m=-l}^l \sqrt{5 \cdot (2l+1) \cdot 5} \begin{pmatrix} 2 & l & 2 \\ 0 & 0 & 0 \end{pmatrix} \left[\begin{pmatrix} 2 & l & 2 \\ +2 & m & M \end{pmatrix} - \begin{pmatrix} 2 & l & 2 \\ -2 & m & M \end{pmatrix} \right] Y_m^{l*}(\hat{q}) Q_l(x), \quad (\text{A.6})$$

$$N_I^{2M,xz} = -2\sqrt{\frac{4\pi}{3}} \sum_{l=0}^3 \sum_{m=-l}^l \sqrt{3 \cdot (2l+1) \cdot 5} \begin{pmatrix} 1 & l & 2 \\ 0 & 0 & 0 \end{pmatrix} \begin{pmatrix} 1 & l & 2 \\ 0 & m & M \end{pmatrix} Y_m^{l*}(\hat{q}) Q_l(x) \hat{q}^z, \quad (\text{A.7})$$

$$S_I^{2M,xz} = 4\sqrt{\frac{4\pi}{30}} \sum_{l=0}^4 \sum_{m=-l}^l \sqrt{5 \cdot (2l+1) \cdot 5} \begin{pmatrix} 2 & l & 2 \\ 0 & 0 & 0 \end{pmatrix} \left[\begin{pmatrix} 2 & l & 2 \\ -1 & m & m \end{pmatrix} - \begin{pmatrix} 2 & l & 2 \\ +1 & m & M \end{pmatrix} \right] Y_m^{l*}(\hat{q}) Q_l(x), \quad (\text{A.8})$$

$$N_I^{2M,yx} = -\sqrt{2}i\sqrt{\frac{4\pi}{3}} \sum_{l=0}^3 \sum_{m=-l}^l \sqrt{3 \cdot (2l+1) \cdot 5} \begin{pmatrix} 1 & l & 2 \\ 0 & 0 & 0 \end{pmatrix} \left[\begin{pmatrix} 1 & l & 2 \\ +1 & m & M \end{pmatrix} + \begin{pmatrix} 1 & l & 2 \\ -1 & m & M \end{pmatrix} \right] Y_m^{l*}(\hat{q}) Q_l(x) \hat{q}^x, \quad (\text{A.9})$$

$$S_I^{2M,yx} = S_I^{2M,xy}, \quad (\text{A.10})$$

$$P_I^{2M,yy} = P_{I;1}^{2M,yy} + P_{I;2}^{2M,yy}, \quad (\text{A.11})$$

where

$$P_{I;1}^{2M,yy} = 0,$$

$$P_{I;2}^{2M,yy} = 4\sqrt{\frac{4\pi}{6}} \frac{k}{|q|} \sum_{l=0}^4 \sum_{m=-l}^l \left\{ \sqrt{\frac{2}{3}} \sqrt{1 \cdot (2l+1) \cdot 5} \begin{pmatrix} 0 & l & 2 \\ 0 & 0 & 0 \end{pmatrix} \begin{pmatrix} 0 & l & 2 \\ 0 & m & M \end{pmatrix} - \frac{1}{\sqrt{5}} \sqrt{5 \cdot (2l+1) \cdot 5} \begin{pmatrix} 2 & l & 2 \\ 0 & 0 & 0 \end{pmatrix} \right. \\ \left. \left[\begin{pmatrix} 2 & l & 2 \\ -2 & m & M \end{pmatrix} + \begin{pmatrix} 2 & l & 2 \\ +2 & m & M \end{pmatrix} + \sqrt{\frac{2}{3}} \begin{pmatrix} 2 & l & 2 \\ 0 & m & M \end{pmatrix} \right] \right\} Y_m^{l*}(\hat{q}) Q_l(x),$$

$$N_I^{2M,yz} = -\sqrt{2}i\sqrt{\frac{4\pi}{3}} \sum_{l=0}^3 \sum_{m=-l}^l \sqrt{3 \cdot (2l+1) \cdot 5} \begin{pmatrix} 1 & l & 2 \\ 0 & 0 & 0 \end{pmatrix} \left[\begin{pmatrix} 1 & l & 2 \\ +1 & m & M \end{pmatrix} + \begin{pmatrix} 1 & l & 2 \\ -1 & m & M \end{pmatrix} \right] Y_m^{l*}(\hat{q}) Q_l(x) \hat{q}^z, \quad (\text{A.12})$$

$$S_I^{2M,yz} = -4i\sqrt{\frac{4\pi}{30}} \frac{k}{|q|} \sum_{l=0}^4 \sum_{m=-l}^l \sqrt{5 \cdot (2l+1) \cdot 5} \begin{pmatrix} 2 & l & 2 \\ 0 & 0 & 0 \end{pmatrix} \left[\begin{pmatrix} 2 & l & 2 \\ -1 & m & M \end{pmatrix} + \begin{pmatrix} 2 & l & 2 \\ +1 & m & M \end{pmatrix} \right] Y_m^{l*}(\hat{q}) Q_l(x) \quad (\text{A.13})$$

$$N_I^{2M,zx} = -2\sqrt{\frac{4\pi}{3}} \sum_{l=0}^3 \sum_{m=-l}^l \sqrt{3 \cdot (2l+1) \cdot 5} \begin{pmatrix} 1 & l & 2 \\ 0 & 0 & 0 \end{pmatrix} \begin{pmatrix} 1 & l & 2 \\ 0 & m & M \end{pmatrix} Y_m^{l*}(\hat{q}) Q_l(x) \hat{q}^x, \quad (\text{A.14})$$

$$S_I^{2M,zz} = S_I^{2M,xz}, \quad (\text{A.15})$$

$$N_I^{2M,zy} = 0, \quad (\text{A.16})$$

$$S_I^{2M,zy} = S_I^{2M,yz}, \quad (\text{A.17})$$

$$P_I^{2M,zz} = P_{I;1}^{2M,zz} + P_{I;2}^{2M,zz}, \quad (\text{A.18})$$

where

$$\begin{aligned} P_{I;1}^{2M,zz} &= -2\sqrt{\frac{4\pi}{3}} \sum_{l=0}^3 \sum_{m=-l}^l \sqrt{3 \cdot (2l+1) \cdot 5} \begin{pmatrix} 1 & l & 2 \\ 0 & 0 & 0 \end{pmatrix} \begin{pmatrix} 1 & l & 2 \\ 0 & m & M \end{pmatrix} Y_m^{l*}(\hat{q}) Q_l(x) \hat{q}^z, \\ P_{I;2}^{2M,zz} &= 4\frac{\sqrt{4\pi}}{3} \frac{k}{|q|} \sum_{l=0}^4 \sum_{m=-l}^l \left\{ \sqrt{1 \cdot (2l+1) \cdot 5} \begin{pmatrix} 0 & l & 2 \\ 0 & 0 & 0 \end{pmatrix} \begin{pmatrix} 0 & l & 2 \\ 0 & m & M \end{pmatrix} \right. \\ &\quad \left. + \frac{2}{\sqrt{5}} \sqrt{5 \cdot (2l+1) \cdot 5} \begin{pmatrix} 2 & l & 2 \\ 0 & 0 & 0 \end{pmatrix} \begin{pmatrix} 2 & l & 2 \\ 0 & m & M \end{pmatrix} \right\} Y_m^{l*}(\hat{q}) Q_l(x), \end{aligned}$$

where $x = \sqrt{1 + m_\pi^2/k^2}$ and Legendre functions of the second kind are given by

$$Q_0(x) = \frac{1}{2} \ln \frac{x+1}{x-1},$$

$$Q_1(x) = \frac{x}{2} \ln \frac{x+1}{x-1} - 1,$$

$$Q_2(x) = \frac{1}{4} (3x^2 - 1) \ln \frac{x+1}{x-1} - \frac{3}{2} x, \quad (\text{A.19})$$

$$Q_3(x) = \frac{2}{3} - \frac{5}{2} x^2 - \frac{1}{4} x (3 - 5x^2) \ln \frac{x+1}{x-1},$$

$$Q_4(x) = \frac{55}{24} x - \frac{35}{8} x^3 + \frac{1}{16} (3 - 30x^2 + 35x^4) \ln \frac{x+1}{x-1}.$$

For type II amplitudes the corresponding tensor components are

$$P_{II}^{2M,x0} = P_{II;1}^{2M,x0} + P_{II;2}^{2M,x0}, \quad (\text{A.20})$$

where

$$\begin{aligned} P_{II;1}^{2M,x0} &= -\sqrt{4\pi} k |q| \frac{x}{\sqrt{6}} \sum_{l=0}^3 \sum_{m=-l}^l \sqrt{3 \cdot (2l+1) \cdot 5} \begin{pmatrix} 1 & l & 2 \\ 0 & 0 & 0 \end{pmatrix} \left[\begin{pmatrix} 1 & l & 2 \\ -1 & m & M \end{pmatrix} - \begin{pmatrix} 1 & l & 2 \\ +1 & m & M \end{pmatrix} \right] Y_m^{l*}(\hat{q}) Q_l(y), \\ P_{II;2}^{2M,x0} &= \frac{k|q|}{3} \sqrt{\frac{1}{10}} \sum_{l=0}^4 \sum_{m=-l}^l \left\{ \sqrt{5 \cdot (2l+1) \cdot 5} \begin{pmatrix} 2 & l & 2 \\ 0 & 0 & 0 \end{pmatrix} \left[\sqrt{6} \left(\rho_{-1} \begin{pmatrix} 2 & l & 2 \\ -2 & m & M \end{pmatrix} - \rho_{+1} \begin{pmatrix} 2 & l & 2 \\ +2 & m & M \end{pmatrix} \right) \right. \right. \\ &\quad \left. \left. + \sqrt{3} \rho_0 \left(\begin{pmatrix} 2 & l & 2 \\ -1 & m & M \end{pmatrix} - \begin{pmatrix} 2 & l & 2 \\ +1 & m & M \end{pmatrix} \right) + 2\rho_{+1} \begin{pmatrix} 2 & l & 2 \\ 0 & m & M \end{pmatrix} \right] \right. \\ &\quad \left. - 2\sqrt{5} \rho_{+1} \sqrt{1 \cdot (2l+1) \cdot 5} \begin{pmatrix} 0 & l & 2 \\ 0 & 0 & 0 \end{pmatrix} \begin{pmatrix} 0 & l & 2 \\ 0 & m & M \end{pmatrix} \right\} Y_m^{l*}(\hat{q}) Q_l(y), \end{aligned}$$

$$P_{II}^{2M,y0} = P_{II;1}^{2M,y0} + P_{II;2}^{2M,y0}, \quad (\text{A.21})$$

where

$$P_{II;1}^{2M,y0} = -i\sqrt{4\pi}k|\mathbf{q}|\frac{x}{\sqrt{6}}\sum_{l=0}^3\sum_{m=-l}^l\sqrt{3\cdot(2l+1)\cdot 5}\begin{pmatrix} 1 & l & 2 \\ 0 & 0 & 0 \end{pmatrix}\left[\begin{pmatrix} 1 & l & 2 \\ +1 & m & M \end{pmatrix}+\begin{pmatrix} 1 & l & 2 \\ -1 & m & M \end{pmatrix}\right]Y_m^{l*}(\hat{q})Q_l(y),$$

$$P_{II;2}^{2M,y0} = \frac{ik|\mathbf{q}|}{3}\sqrt{\frac{1}{10}}\sum_{l=0}^4\sum_{m=-l}^l\left\{\sqrt{5\cdot(2l+1)\cdot 5}\begin{pmatrix} 2 & l & 2 \\ 0 & 0 & 0 \end{pmatrix}\right.$$

$$\left. \left[\sqrt{6}\left(\rho_{+1}\begin{pmatrix} 2 & l & 2 \\ +2 & m & M \end{pmatrix}+\rho_{-1}\begin{pmatrix} 2 & l & 2 \\ -2 & m & M \end{pmatrix}\right)+\sqrt{3}\rho_0\left(\begin{pmatrix} 2 & l & 2 \\ +1 & m & M \end{pmatrix}+\begin{pmatrix} 2 & l & 2 \\ -1 & m & M \end{pmatrix}\right)\right]Y_m^{l*}(\hat{q})Q_l(y),$$

$$P_{II}^{2M,z0} = P_{II;1}^{2M,z0} + P_{II;2}^{2M,z0}, \quad (\text{A.22})$$

where

$$P_{II;1}^{2M,z0} = -\sqrt{4\pi}k|\mathbf{q}|\frac{x}{\sqrt{3}}\sum_{l=0}^3\sum_{m=-l}^l\sqrt{3\cdot(2l+1)\cdot 5}\begin{pmatrix} 1 & l & 2 \\ 0 & 0 & 0 \end{pmatrix}\begin{pmatrix} 1 & l & 2 \\ 0 & m & M \end{pmatrix}Y_m^{l*}(\hat{q})Q_l(y),$$

$$P_{II;2}^{2M,z0} = \frac{k|\mathbf{q}|}{3}\sqrt{\frac{1}{5}}\sum_{l=0}^4\sum_{m=-l}^l\left\{\sqrt{5\cdot(2l+1)\cdot 5}\begin{pmatrix} 2 & l & 2 \\ 0 & 0 & 0 \end{pmatrix}\left[\sqrt{3}\left(\rho_{-1}\begin{pmatrix} 2 & l & 2 \\ -1 & m & M \end{pmatrix}+\rho_{+1}\begin{pmatrix} 2 & l & 2 \\ +1 & m & M \end{pmatrix}\right)\right.\right.$$

$$\left. \left.+2\rho_0\begin{pmatrix} 2 & l & 2 \\ 0 & m & M \end{pmatrix}\right]+\sqrt{1\cdot(2l+1)\cdot 5}\begin{pmatrix} 0 & l & 2 \\ 0 & 0 & 0 \end{pmatrix}\rho_0\begin{pmatrix} 0 & l & 2 \\ 0 & m & M \end{pmatrix}\right\}Y_m^{l*}(\hat{q})Q_l(y),$$

$$P_{II}^{2M,xx} = P_{II;1}^{2M,xx} + P_{II;2}^{2M,xx} + P_{II;3}^{2M,xx} + P_{II;4}^{2M,xx} + P_{II;5}^{2M,xx}, \quad (\text{A.23})$$

where

$$P_{II;1}^{2M,xx} = \sqrt{4\pi}[x(x^2+1)k^2 - m_\pi^2x + x^2|\mathbf{q}|k]Y_M^{2*}(\hat{q})Q_2(y),$$

$$P_{II;2}^{2M,xx} = -\sqrt{\frac{4\pi}{3}}[k^2(x^2+1) + m_\pi^2]\sum_{l=0}^3\sum_{m=-l}^l\sqrt{3\cdot(2l+1)\cdot 5}\begin{pmatrix} 1 & l & 2 \\ 0 & 0 & 0 \end{pmatrix}$$

$$\left[\rho_{-1}\begin{pmatrix} 1 & l & 2 \\ -1 & m & M \end{pmatrix}+\rho_0\begin{pmatrix} 1 & l & 2 \\ 0 & m & M \end{pmatrix}+\rho_{+1}\begin{pmatrix} 1 & l & 2 \\ +1 & m & N \end{pmatrix}\right]Y_m^{l*}(\hat{q})Q_l(y),$$

$$P_{II;3}^{2M,xx} = -\sqrt{4\pi}\frac{k|\mathbf{q}|}{3}\left\{\sum_{l=0}^4\sum_{m=-l}^l\left\{\sqrt{\frac{2}{5}}\sqrt{5\cdot(2l+1)\cdot 5}\begin{pmatrix} 2 & l & 2 \\ 0 & 0 & 0 \end{pmatrix}\right.\right.$$

$$\left.\left[\sqrt{3}\left(\rho_{-1}^2\begin{pmatrix} 2 & l & 2 \\ -2 & m & M \end{pmatrix}+\rho_{+1}^2\begin{pmatrix} 2 & l & 2 \\ +2 & m & M \end{pmatrix}\right)+\sqrt{6}\rho_0\left(\rho_{-1}\begin{pmatrix} 2 & l & 2 \\ -1 & m & M \end{pmatrix}+\rho_{+1}\begin{pmatrix} 2 & l & 2 \\ +1 & m & M \end{pmatrix}\right)\right.\right.$$

$$\left. \left.+ \sqrt{2}(\rho_0^2 + \rho_{-1}\rho_{+1})\begin{pmatrix} 2 & l & 2 \\ 0 & m & M \end{pmatrix}\right]+\sqrt{1\cdot(2l+1)\cdot 5}\begin{pmatrix} 0 & l & 2 \\ 0 & 0 & 0 \end{pmatrix}\begin{pmatrix} 0 & l & 2 \\ 0 & m & M \end{pmatrix}\right\}Y_m^{l*}(\hat{q})Q_l(y)\Big\},$$

$$P_{II;4}^{2M,xx} = P_{II;4a}^{2M,xx} + P_{II;4b}^{2M,xx},$$

and

$$P_{II;4a}^{2M,xx} = k\sqrt{\frac{4\pi}{6}}(2kx^2 - |\mathbf{q}|x) \sum_{l=0}^3 \sum_{m=-l}^l \sqrt{3 \cdot (2l+1) \cdot 5} \begin{pmatrix} 1 & l & 2 \\ 0 & 0 & 0 \end{pmatrix} \left[\begin{pmatrix} 1 & l & 2 \\ -1 & m & m \end{pmatrix} - \begin{pmatrix} 1 & l & 2 \\ +1 & m & M \end{pmatrix} \right] Y_m^{l*}(\hat{q}) Q_l(y) \hat{q}^x,$$

$$P_{II;4b}^{2M,xx} = \sqrt{4\pi} \frac{k|\mathbf{q}|}{3\sqrt{2}} \left\{ \sum_{l=0}^4 \sum_{m=-l}^l \left\{ \frac{1}{\sqrt{5}} \sqrt{5 \cdot (2l+1) \cdot 5} \begin{pmatrix} 2 & l & 2 \\ 0 & 0 & 0 \end{pmatrix} \right. \right. \\ \left. \left[\sqrt{6} \left(\rho_{-1} \begin{pmatrix} 2 & l & 2 \\ -2 & m & M \end{pmatrix} - \rho_{+1} \begin{pmatrix} 2 & l & 2 \\ +2 & m & M \end{pmatrix} \right) + \sqrt{3} \rho_0 \left(\begin{pmatrix} 2 & l & 2 \\ -1 & m & M \end{pmatrix} - \begin{pmatrix} 2 & l & 2 \\ +1 & m & M \end{pmatrix} \right) \right. \right. \\ \left. \left. + (\rho_{+1} - \rho_{-1}) \begin{pmatrix} 2 & l & 2 \\ 0 & m & M \end{pmatrix} \right] - (\rho_{+1} - \rho_{-1}) \sqrt{1 \cdot (2l+1) \cdot 5} \begin{pmatrix} 0 & l & 2 \\ 0 & m & 0 \end{pmatrix} \begin{pmatrix} 0 & l & 2 \\ 0 & m & M \end{pmatrix} \right\} Y_m^{l*}(\hat{q}) Q_l(y) \hat{q}^x \right\},$$

$$P_{II;5}^{2M,xx} = -\sqrt{4\pi} k^2 \left\{ \sum_{l=0}^4 \sum_{m=-l}^l \left\{ \frac{2}{3} \sqrt{1 \cdot (2l+1) \cdot 5} \begin{pmatrix} 0 & l & 2 \\ 0 & 0 & 0 \end{pmatrix} \begin{pmatrix} 0 & l & 2 \\ 0 & m & M \end{pmatrix} \right. \right. \\ \left. \left. + \sqrt{\frac{2}{15}} \sqrt{5 \cdot (2l+1) \cdot 5} \begin{pmatrix} 2 & l & 2 \\ 0 & 0 & 0 \end{pmatrix} \left[\begin{pmatrix} 2 & l & 2 \\ -2 & m & M \end{pmatrix} + \begin{pmatrix} 2 & l & 2 \\ +2 & m & M \end{pmatrix} - \sqrt{\frac{2}{3}} \begin{pmatrix} 2 & l & 2 \\ 0 & m & M \end{pmatrix} \right] \right\} Y_m^{l*}(\hat{q}) Q_l(y) \right\},$$

$$N_{II}^{2M,xy} = 0, \quad (\text{A.24})$$

$$S_{II}^{2M,xy} = -i\sqrt{4\pi} k^2 \sqrt{\frac{2}{15}} \sum_{l=0}^4 \sum_{m=-l}^l \sqrt{5 \cdot (2l+1) \cdot 5} \begin{pmatrix} 2 & l & 2 \\ 0 & 0 & 0 \end{pmatrix} \left[\begin{pmatrix} 2 & l & 2 \\ +2 & m & M \end{pmatrix} - \begin{pmatrix} 2 & l & 2 \\ -2 & m & M \end{pmatrix} \right] Y_m^{l*}(\hat{q}) Q_l(y), \quad (\text{A.25})$$

$$N_{II}^{2M,xz} = N_{II;1}^{2M,xz} + N_{II;2}^{2M,xz}, \quad (\text{A.26})$$

where

$$N_{II;1}^{2M,xz} = \sqrt{\frac{4\pi}{6}} k(2kx^2 - |\mathbf{q}|x) \sum_{l=0}^3 \sum_{m=-l}^l \sqrt{3 \cdot (2l+1) \cdot 5} \begin{pmatrix} 1 & l & 2 \\ 0 & 0 & 0 \end{pmatrix} \left[\begin{pmatrix} 1 & l & 2 \\ -1 & m & M \end{pmatrix} - \begin{pmatrix} 1 & l & 2 \\ +1 & m & M \end{pmatrix} \right] Y_m^{l*}(\hat{q}) Q_l(y) \hat{q}^z,$$

$$N_{II;2}^{2M,xz} = \sqrt{\frac{4\pi}{3}} \frac{k|\mathbf{q}|}{\sqrt{6}} \left\{ \sum_{l=0}^4 \sum_{m=-l}^l \left\{ \frac{1}{\sqrt{5}} \sqrt{5 \cdot (2l+1) \cdot 5} \begin{pmatrix} 2 & l & 2 \\ 0 & 0 & 0 \end{pmatrix} \right. \right. \\ \left. \left[\sqrt{6} \left(\rho_{-1} \begin{pmatrix} 2 & l & 2 \\ -2 & m & M \end{pmatrix} - \rho_{+1} \begin{pmatrix} 2 & l & 2 \\ +2 & m & M \end{pmatrix} \right) + \sqrt{3} \rho_0 \left(\begin{pmatrix} 2 & l & 2 \\ -1 & m & M \end{pmatrix} - \begin{pmatrix} 2 & l & 2 \\ +1 & m & M \end{pmatrix} \right) \right. \right. \\ \left. \left. + (\rho_{+1} - \rho_{-1}) \begin{pmatrix} 2 & l & 2 \\ 0 & m & M \end{pmatrix} \right] - (\rho_{+1} - \rho_{-1}) \sqrt{1 \cdot (2l+1) \cdot 5} \begin{pmatrix} 0 & l & 2 \\ 0 & 0 & 0 \end{pmatrix} \begin{pmatrix} 0 & l & 2 \\ 0 & m & M \end{pmatrix} \right\} Y_m^{l*}(\hat{q}) Q_l(y) \right\} \hat{q}^z,$$

$$S_{II}^{2M,xz} = -\sqrt{\frac{4\pi}{3}} \sqrt{\frac{2}{5}} x k^2 \sum_{l=0}^4 \sum_{m=-l}^l \sqrt{5 \cdot (2l+1) \cdot 5} \begin{pmatrix} 2 & l & 2 \\ 0 & 0 & 0 \end{pmatrix} \left[\begin{pmatrix} 2 & l & 2 \\ -1 & m & M \end{pmatrix} - \begin{pmatrix} 2 & l & 2 \\ +1 & m & M \end{pmatrix} \right] Y_m^{l*}(\hat{q}) Q_l(y), \quad (\text{A.27})$$

$$N_{II}^{2M,yx} = N_{II;1}^{2M,yx} + N_{II;2}^{2M,yx}, \quad (\text{A.28})$$

where

$$N_{II;1}^{2M,yx} = \sqrt{4\pi} \frac{ik(2kx^2 - |\mathbf{q}|x)}{\sqrt{6}} \sum_{l=0}^3 \sum_{m=-l}^l \sqrt{3 \cdot (2l+1) \cdot 5} \begin{pmatrix} 1 & l & 2 \\ 0 & 0 & 0 \end{pmatrix} \left[\begin{pmatrix} 1 & l & 2 \\ +1 & m & M \end{pmatrix} + \begin{pmatrix} 1 & l & 2 \\ -1 & m & M \end{pmatrix} \right] Y_m^{l*}(\hat{q}) Q_l(y) \hat{q}^x,$$

$$\begin{aligned}
N_{II;2}^{2M,yx} &= \sqrt{4\pi} \frac{ik|\mathbf{q}|}{\sqrt{30}} \sum_{l=0}^4 \sum_{m=-l}^l \sqrt{5 \cdot (2l+1) \cdot 5} \begin{pmatrix} 2 & l & 2 \\ 0 & 0 & 0 \end{pmatrix} \\
&\quad \left[\rho_0 \left(\begin{pmatrix} 2 & l & 2 \\ +1 & m & M \end{pmatrix} + \begin{pmatrix} 2 & l & 2 \\ -1 & m & M \end{pmatrix} \right) + \sqrt{2} \left(\rho_{+1} \begin{pmatrix} 2 & l & 2 \\ +2 & m & M \end{pmatrix} + \rho_{-1} \begin{pmatrix} 2 & l & 2 \\ -2 & m & M \end{pmatrix} \right) \right] Y_m^{l*}(\hat{q}) Q_l(y) \hat{q}^x, \\
S_{II}^{2M,yx} &= S_{II}^{2M,xy},
\end{aligned} \tag{A.29}$$

$$P_{II}^{2M,yy} = P_{II;1}^{2M,yy} + P_{II;2}^{2M,yy} + P_{II;3}^{2M,yy} + P_{II;4}^{2M,yy} + P_{II;5}^{2M,yy}, \tag{A.30}$$

where

$$P_{II;1}^{2M,yy} = P_{II;1}^{2M,xx}, \quad P_{II;2}^{2M,yy} = P_{II;2}^{2M,xx}, \quad P_{II;3}^{2M,yy} = P_{II;3}^{2M,xx},$$

$$P_{II;4}^{2M,yy} = 0,$$

$$\begin{aligned}
P_{II;5}^{2M,yy} &= -\sqrt{4\pi} \sqrt{\frac{2}{3}} x k^2 \left\{ \sum_{l=0}^4 \sum_{m=-l}^l \left\{ \sqrt{\frac{2}{3}} \sqrt{1 \cdot (2l+1) \cdot 5} \begin{pmatrix} 0 & l & 2 \\ 0 & 0 & 0 \end{pmatrix} \begin{pmatrix} 0 & l & 2 \\ 0 & m & M \end{pmatrix} \right. \right. \\
&\quad \left. \left. - \frac{1}{\sqrt{5}} \sqrt{5 \cdot (2l+1) \cdot 5} \begin{pmatrix} 2 & l & 2 \\ 0 & 0 & 0 \end{pmatrix} \left[\begin{pmatrix} 2 & l & 2 \\ -2 & m & M \end{pmatrix} + \begin{pmatrix} 2 & l & 2 \\ +2 & m & M \end{pmatrix} + \sqrt{\frac{2}{3}} \begin{pmatrix} 2 & l & 2 \\ 0 & m & M \end{pmatrix} \right] \right\} Y_m^{l*}(\hat{q}) Q_l(y) \right\}, \\
N_{II}^{2M,yz} &= N_{II;1}^{2M,yz} + N_{II;2}^{2M,yz},
\end{aligned} \tag{A.31}$$

where

$$\begin{aligned}
N_{II;1}^{2M,yz} &= \sqrt{4\pi} \frac{ik(2kx^2 - |\mathbf{q}x|)}{\sqrt{6}} \sum_{l=0}^3 \sum_{m=-l}^l \sqrt{3 \cdot (2l+1) \cdot 5} \begin{pmatrix} 1 & l & 2 \\ 0 & 0 & 0 \end{pmatrix} \left[\begin{pmatrix} 1 & l & 2 \\ +1 & m & M \end{pmatrix} + \begin{pmatrix} 1 & l & 2 \\ -1 & m & M \end{pmatrix} \right] Y_m^{l*}(\hat{q}) Q_l(y) \hat{q}^z, \\
N_{II;2}^{2M,yz} &= \sqrt{4\pi} \frac{ik|\mathbf{q}|}{\sqrt{30}} \sum_{l=0}^4 \sum_{m=-l}^l \sqrt{5 \cdot (2l+1) \cdot 5} \begin{pmatrix} 2 & l & 2 \\ 0 & 0 & 0 \end{pmatrix} \\
&\quad \left[\rho_0 \left(\begin{pmatrix} 2 & l & 2 \\ +1 & m & M \end{pmatrix} + \begin{pmatrix} 2 & l & 2 \\ -1 & m & M \end{pmatrix} \right) + \sqrt{2} \left(\rho_{+1} \begin{pmatrix} 2 & l & 2 \\ +2 & m & M \end{pmatrix} + \rho_{-1} \begin{pmatrix} 2 & l & 2 \\ -2 & m & M \end{pmatrix} \right) \right] Y_m^{l*}(\hat{q}) Q_l(y) \hat{q}^z, \\
S_{II}^{2M,yz} &= \sqrt{\frac{4\pi}{3}} \sqrt{\frac{2}{5}} i k^2 x \sum_{l=0}^4 \sum_{m=-l}^l \sqrt{5 \cdot (2l+1) \cdot 5} \begin{pmatrix} 2 & l & 2 \\ 0 & 0 & 0 \end{pmatrix} \left[\begin{pmatrix} 2 & l & 2 \\ -1 & m & M \end{pmatrix} + \begin{pmatrix} 2 & l & 2 \\ +1 & m & M \end{pmatrix} \right] Y_m^{l*}(\hat{q}) Q_l(y), \\
N_{II}^{2M,zx} &= N_{II;1}^{2M,zx} + N_{II;2}^{2M,zx},
\end{aligned} \tag{A.32}$$

where

$$\begin{aligned}
N_{II;1}^{2M,zx} &= \sqrt{\frac{4\pi}{3}} k (2kx^2 - |\mathbf{q}x|) \sum_{l=0}^3 \sum_{m=-l}^l \sqrt{3 \cdot (2l+1) \cdot 5} \begin{pmatrix} 1 & l & 2 \\ 0 & 0 & 0 \end{pmatrix} \begin{pmatrix} 1 & l & 2 \\ 0 & m & M \end{pmatrix} Y_m^{l*}(\hat{q}) Q_l(y) \hat{q}^x, \\
N_{II;2}^{2M,zx} &= \frac{\sqrt{4\pi}}{3} k |\mathbf{q}| \left\{ \sum_{l=0}^4 \sum_{m=-l}^l \left\{ \frac{1}{\sqrt{5}} \sqrt{5 \cdot (2l+1) \cdot 5} \begin{pmatrix} 2 & l & 2 \\ 0 & 0 & 0 \end{pmatrix} \right. \right. \\
&\quad \left[\sqrt{3} \left(\rho_{-1} \begin{pmatrix} 2 & l & 2 \\ -1 & m & M \end{pmatrix} + \rho_{+1} \begin{pmatrix} 2 & l & 2 \\ +1 & m & M \end{pmatrix} \right) + 2\rho_0 \begin{pmatrix} 2 & l & 2 \\ 0 & m & M \end{pmatrix} \right] \\
&\quad \left. \left. + \rho_0 \sqrt{1 \cdot (2l+1) \cdot 5} \begin{pmatrix} 0 & l & 2 \\ 0 & 0 & 0 \end{pmatrix} \right\} Y_m^{l*}(\hat{q}) Q_l(y) \right\} \hat{q}^x,
\end{aligned}$$

$$S_{II}^{2M,zz} = S_{II}^{2M,xz}, \quad (\text{A.34})$$

$$N_{II}^{2M,zy} = 0, \quad (\text{A.35})$$

$$S_{II}^{2M,zy} = S_{II}^{2M,yz}, \quad (\text{A.36})$$

$$P_{II}^{2M,zz} = P_{II;1}^{2M,zz} + P_{II;2}^{2M,zz} + P_{II;3}^{2M,zz} + P_{II;4}^{2M,zz} + P_{II;5}^{2M,zz}, \quad (\text{A.37})$$

where

$$P_{II;1}^{2M,zz} = P_{II;1}^{2M,xx}, \quad P_{II;2}^{2M,zz} = P_{II;2}^{2M,xx}, \quad P_{II;3}^{2M,zz} = P_{II;3}^{2M,xx},$$

$$P_{II;4}^{2M,zz} = P_{II;4a}^{2M,zz} + P_{II;4b}^{2M,zz},$$

$$P_{II;4a}^{2M,zz} = \sqrt{\frac{4\pi}{3}} k(2kx^2 - |\mathbf{q}|x) \sum_{l=0}^3 \sum_{m=-l}^l \sqrt{3 \cdot (2l+1) \cdot 5} \begin{pmatrix} 1 & l & 2 \\ 0 & 0 & 0 \end{pmatrix} \begin{pmatrix} 1 & l & 2 \\ 0 & m & M \end{pmatrix} Y_m^l(\hat{q}) Q_l(y) \hat{q}^z,$$

$$P_{II;4b}^{2M,zz} = \frac{\sqrt{4\pi}}{3} k|\mathbf{q}| \left\{ \sum_{l=0}^4 \sum_{m=-l}^l \left\{ \frac{1}{\sqrt{5}} \sqrt{5 \cdot (2l+1) \cdot 5} \begin{pmatrix} 2 & l & 2 \\ 0 & 0 & 0 \end{pmatrix} \right. \right. \\ \left. \left[\sqrt{3} \left(\rho_{-1} \begin{pmatrix} 2 & l & 2 \\ -1 & m & M \end{pmatrix} + \rho_{+1} \begin{pmatrix} 2 & l & 2 \\ +1 & m & M \end{pmatrix} \right) + 2\rho_0 \begin{pmatrix} 2 & l & 2 \\ 0 & m & M \end{pmatrix} \right] \right. \\ \left. \left. + \rho_0 \sqrt{1 \cdot (2l+1) \cdot 5} \begin{pmatrix} 0 & l & 2 \\ 0 & 0 & 0 \end{pmatrix} \begin{pmatrix} 0 & l & 2 \\ 0 & m & M \end{pmatrix} \right\} Y_m^l(\hat{q}) Q_l(y) \right\} \hat{q}^z,$$

$$P_{II;5}^{2M,zz} = -\sqrt{4\pi} \frac{2}{3} xk^2 \left\{ \sum_{l=0}^4 \sum_{m=-l}^l \left\{ \sqrt{1 \cdot (2l+1) \cdot 5} \begin{pmatrix} 0 & l & 2 \\ 0 & 0 & 0 \end{pmatrix} \begin{pmatrix} 0 & l & 2 \\ 0 & m & M \end{pmatrix} \right. \right. \\ \left. \left. + \frac{2}{\sqrt{5}} \sqrt{5 \cdot (2l+1) \cdot 5} \begin{pmatrix} 2 & l & 2 \\ 0 & 0 & 0 \end{pmatrix} \begin{pmatrix} 2 & l & 2 \\ 0 & m & M \end{pmatrix} \right\} Y_m^l(\hat{q}) Q_l(y) \right\}.$$

where for particle a exchanged in the upper part of diagrams shown in Fig. 2

$$y = x + \frac{m_a^2 - m_\pi^2}{2|\mathbf{q}|k}. \quad (\text{A.38})$$

The coefficients ρ_{-1} , ρ_0 and ρ_{+1} are used in the expansion of the product $\hat{q} \cdot \hat{\kappa}$ in terms of spherical harmonics:

$$\hat{q} \cdot \hat{\kappa} = \sqrt{\frac{4\pi}{3}} \sum_{m=-1}^{+1} \rho_m Y_m^1(\Omega) \quad (\text{A.39})$$

and can be expressed by the angle between photon momentum and spin quantisation axis as $\rho_0 = \cos \theta_q$, $\rho_{\pm 1} = \pm \sin \theta_q / \sqrt{2}$.

- [3] M. A. Pichowsky, T.-S. H. Lee, Phys. Rev. D **56**, 1644 (1997)
- [4] B. Friman, M. Soyeur, Nucl. Phys. A **600**, 477 (1996)
- [5] Y. Oh, T.-S. H. Lee, Phys. Rev. C **69**, 025201 (2004)
- [6] J.A. Gómez Tejedor, E. Oset, Nucl. Phys. A **571**, 667 (1994)
- [7] J.A. Gómez Tejedor, E. Oset, Nucl. Phys. A **600**, 413 (1996)
- [8] J.C. Nacher, E. Oset, M.J. Vicente Vacas, L. Roca, Nucl. Phys. A **695** (2001)
- [9] M. Battaglieri et al., Phys. Rev. D **80**, 072005 (2009)
- [10] A. Airapetian et al., Phys. Lett. B **599**, 212 (2004)
- [11] Ł. Bibrzycki, L. Leśniak, A. P. Szczepaniak, Eur. Phys. J. C **34**, 335 (2004)
- [12] Ł. Bibrzycki, L. Leśniak, EPJ Web Conf. **37**, 09009 (2012)
- [13] B. Renner, Nucl. Phys. B **30**, 634 (1971)
- [14] M. Suzuki, Phys. Rev. D **47**, 1043 (1993)
- [15] E. Triantafillopoulos, Lett. Nuovo Cim. **39**, 1 (1984)
- [16] A. Ahmadzadeh, R. J. Jacob, Phys. Rev. **160**, 1359 (1967)
- [17] D. Toublan, Phys. Rev D **53**, 6602 (1996)
- [18] F. Giacosa, T. Gutsche, V. E. Lyubovitskij and A. Faessler, Phys. Rev. D **72**, 114021 (2005)
- [19] N.N. Achasov, G.N. Shestakov, Phys. Rev. D **77**, 074020 (2008)
- [20] N.N. Achasov, G.N. Shestakov, Phys. Usp. **54**, 799 (2011)
- [21] T. Mori *et al.* (Belle Collaboration), Phys. Rev. D **75**, 051101 (2007)
- [22] Ch-R Ji, R. Kamiński, L. Leśniak, A. Szczepaniak, R. Williams, Phys. Rev. C **58**, 1205 (1998)
- [23] L. Leśniak, A.P. Szczepaniak, Acta Phys. Pol. B **34**, 3389 (2003)
- [24] R. Garcia-Martin, R. Kamiński, J.R. Pelaez, J. Ruiz de Elvira and F.J. Yndurain, Phys. Rev. D **83**, 074004 (2011)
- [25] R. Kamiński, Phys. Rev. D **83**, 076008 (2011)
- [26] R. Machleidt, K. Holinde, Ch. Elster, Phys. Rep. **149**, 1 (1987)
- [27] Ł. Bibrzycki, R. Kamiński, in preparation.
- [28] J. Ballam *et al.*, Phys. Rev. D **5**, 545 (1972)
- [29] A. J. Pawlicki *et al.*, Phys. Rev. D **15**, 3196 (1977)
- [30] S. Weinberg, Phys. Rev. **133**, B1318 (1964)